Upscaling of methane exchange in a boreal forest using soil chamber measurements and high-resolution LiDAR elevation data

E. Sundqvist[1], A Persson[1], N. Kljun[2, 3], P. Vestin[1], L. Chasmer[4], C.Hopkinson[4], A. Lindroth[1]

[1]Department of Physical Geography and Ecosystem Science, Lund University, Sweden

[2] Department of Geography, Swansea University, United Kingdom

[3] Centre for Studies of Carbon Cycle and Climate Interactions (LUCCI), Department of Physical Geography and Ecosystem Science, Lund University, Sweden

[4] Department of Geography, University of Lethbridge, Alberta, Canada

Corresponding author:

Elin Sundqvist

Department of physical geography and ecosystem science, Lund University

Sölvegatan 12

223 62 Lund

Sweden

Phone: +46 46 2229759

Email: elin.sundqvist@nateko.lu.se

Abstract

Forest soils are generally considered to be net sinks of methane (CH_4), but CH_4 fluxes vary spatially depending on soil conditions. Measuring CH_4 exchange with chambers, which are commonly used for this purpose, might not result in representative fluxes at site scale. Appropriate methods for upscaling CH_4 fluxes from point measurements to site scale are therefore needed. At the boreal forest research site, Norunda, chamber measurements of soils and vegetation indicate that the site is a net sink of CH_4, while tower gradient measurements indicate that the site is a net source of CH_4. We investigated the discrepancy between chamber and tower gradient measurements by upscaling soil CH_4 exchange to a 100 ha area based on an empirical model derived from chamber measurements of CH_4 exchange and measurements of soil moisture, soil temperature and water table depth. A digital elevation model (DEM) derived from high-resolution airborne Light Detection And Ranging (LiDAR) data was used to generate gridded water table depth and soil moisture data of the study area as input data for the upscaling. Despite the simplistic approach, modeled fluxes were significantly correlated to four out of five chambers with $R > 0.68$. The upscaling resulted in a net soil sink of CH_4 of -10μmol $m^{-2}h^{-1}$, averaged over the entire study area and time period (June-September, 2010). Our findings suggests that additional contributions from CH_4 soil sources outside the upscaling study area and possibly CH_4 emissions from vegetation could explain the net emissions measured by tower gradient measurements.

Keywords: methane (CH_4) fluxes, water table depth, topographic wetness index, soil moisture, soil temperature, methane consumption

1. Introduction

The only well characterized biospheric sink for CH_4 is oxidation by methanotrophic bacteria in soil (Harriss et al., 1982). Globally, this soil CH_4 sink was estimated to range between 28 and 32 Tg CH_4 yr^{-1}, which amounts to around 5% of the destruction of CH_4 by OH radicals in the troposphere (Kirschke, 2013). Forest soils are generally considered to be net sinks of CH_4 with higher uptake rates than grassland and arable land (Boeckx et al., 1997; Dutaur and Verchot, 2007). However, CH_4 production by archeans usually dominates in anaerobic forest soil environments such as waterlogged soils (Christiansen et al., 2012; Jungkunst et al., 2008; McNamara et al., 2006). CH_4 production also takes place in well-aerated soils at anaerobic micro sites (Fischer and Hedin, 2002; Kammann et al., 2009) and in deeper soil layers where anaerobic conditions occur (Kammann et al., 2001). Hence consumption and production can occur simultaneously at one location and soil conditions will determine the direction of the net flux. Vegetation might also contribute to the CH_4 exchange of a forest. Trees have been found to transport CH_4 originating from soil water and to release it through the stem or foliage (Terazawa et al. 2007; Gauci 2010). Aerobic formation of CH_4 in green plants has also been observed (Keppler et al. 2006; Vigano et al. 2008), although the mechanisms governing plant CH_4 release are still discussed (Bruhn et al., 2012) and there is little evidence of plant emissions of CH_4 from in-situ studies (Sundqvist et al., 2012). On the contrary, Sundqvist et al. (2012) found evidence for plant uptake of atmospheric CH_4 from measurements on spruce, pine, birch and rowan in a boreal forest.

Soil CH_4 flux rates also vary considerably both spatially and temporally (Christiansen et al., 2012; Ishizuka et al., 2009; Konda et al., 2008; Lessard et al., 1994; Reay et al., 2005; Yu et al., 2008). Spatial variability in soil CH_4 fluxes can be due to variability in soil moisture, soil

texture, and water table depths, factors that are dependent on topography, vegetation, and soil type, for example. Soil moisture (Castro et al., 1994; Guckland et al., 2009; Lessard et al., 1994) and soil texture (Dorr et al., 1993; Dutaur and Verchot, 2007; Ishizuka et al., 2009) alters soil diffusivity, which controls the rate at which atmospheric CH_4, and oxygen are supplied to the bacteria. Water table depth alters the relative extent of aerobic and anaerobic zones in soils. A rise of the water table leads to a decreased oxic soil zone and thus reduced CH_4 uptake (Kammann et al., 2001; Roulet et al., 1992). Changes in soil temperature and precipitation are also responsible for temporal variability in CH_4 exchange. Increases in temperature stimulate the activity of both methanogens (Yvon-Durocher et al., 2014) and methanotrophs (Crill et al., 1994; King and Adamsen, 1992), although methanogens benefit more (Dunfield et al., 1993). Other factors that have been found to influence soil CH_4 exchange in forests are soil pH (Weslien et al., 2009) and nitrogen availability (Steudler et al., 1989).

In situ chamber measurements and soil incubations in laboratories have long been the dominant methods for studying CH_4 exchange in forests, although larger scale micrometeorological methods are gaining in popularity (Nicoloni et al., 2013). While CH_4 exchange occurs and is often measured at the centimeter scale, it varies globally, and has a significant influence on biospheric-atmospheric interactions and feedbacks associated with climatic change (Schimel and Potter, 1995). Appropriate upscaling of CH_4 exchange from chamber-based point measurements will allow scientists to better understand the contribution of methane from soil and plant environments measured using eddy covariance/micrometeorological methods with extension to model estimates of regional to global CH_4 budgets (Hashimoto et al., 2011; Marushchak et al., 2013; Schimel and Potter, 1995). A few studies have upscaled CH_4 fluxes using simple extrapolations of chamber measurements or soil incubations from a few

92 locations multiplied by site area. However these methods do not consider the spatial
93 heterogeneity of forest soil texture or type, or topographical variability, which may greatly
94 influence wetting and drying regimes, and therefore CH_4 fluxes.
95 Global and regional estimates of soil CH_4 sink strength use soil texture classes (Dorr et al., 1993;
96 Dutaur and Verchot, 2007), land use type (Grunwald et al., 2012), ecosystem class and/or
97 climatic zones (Dutaur and Verchot, 2007) to spatially parameterize CH_4 exchanges. However,
98 regional models often fail to incorporate the spatial heterogeneity within each class, including
99 fuzzy boundaries between classes. This results in inaccurate characterization of classes, and
100 especially within the sometimes broad transition zones between classes (Matson et al., 1989).
101 These issues may be overcome by incorporating process-based models of CH_4 consumption
102 driven by gaseous diffusion or diffusion in combination with microbial activity (Curry, 2007;
103 Del Grosso et al., 2000; Ridgwell et al., 1999). Some process-based models do not account for
104 production of CH_4 and are not applicable to soils that seasonally shift from net sinks to net
105 sources (Del Grosso et al., 2000). Process-based models can become exceedingly complex,
106 requiring detailed inputs of spatio-temporally varying climate, vegetation and soil
107 physiochemical properties (Hashimoto et al., 2011). More simple, empirical models have been
108 developed for site-specific applications. Castro et al (1994) found that soil moisture, as the only
109 explanatory variable, could satisfactorily predict CH_4 fluxes at locations within a temperate
110 forest. Christiansen et al. (2012) used spatial variability in soil moisture and water table depths
111 derived from elevation data to upscale CH_4 fluxes from manual chamber measurements to site
112 scale at two temperate deciduous forests.
113 At the Norunda boreal forest site in central Sweden, chamber measurements of soils and
114 vegetation indicate that the site is a net sink of CH_4 (Sundqvist et al., 2012, 2014b), while

gradient measurements above the forest canopy indicate that the site is a net source of CH_4 (Sundqvist et al., 2015). The aim of this study was to quantify soil CH_4 exchange for the entire site (100 ha) by upscaling soil CH_4 exchange through developing an empirical model for a mature coniferous forest based on automated chamber observations with a high temporal resolution, in combination with high-resolution LiDAR elevation data. The model will also serve as a mean to further examine the discrepancy between results obtained from chamber measurements and tower gradient measurements. In correspondence to findings of Christiansen et al. (2012), Fiedler et al. (2005) and Grunwald et al. (2012), we hypothesize that emissions from wet patches scattered at the site may exceed the uptake in well-aerated parts of the soil and hence even relatively small source areas may shift a larger area from a sink to a source (Fiedler et al., 2005).

2. Method

2.1 Site description

Upscaling of soil CH_4 exchange was completed for a 100 ha area at the Norunda site, 60˚5′N, 17˚29′E, in central Sweden from July through September 2010 during coincident chamber and tower gradient measurements. The Norunda site is situated at the southern edge of the boreal forest zone and is comprised of 120 years old mixed pine (Pinus sylvestris) and spruce (Picea abies) trees. The forest was thinned in 2008 within the NE to SW sectors surrounding the measurement tower to a radius of 200 m, which decreased the leaf area index within this area from 4.8 to 2.8 m^2m^{-2}. Trees within the SW to NE sectors have not been thinned nor fertilized in the last few decades. Soil are comprised of glacial till, classified as dystric regosol (Lundin et al., 1999) and include an organic layer of about 3-10 cm. The area within 500 m radius of the measurement tower is relatively flat, with elevation ranges from 40-52 m above sea level (Figure 1). Since 1843, the water table in the area has been artificially lowered as a result of several ditches surrounding the forest. The last known ditch installation was in 1980. Mean air temperature measured at Uppsala climate station, 30 km south of Norunda, was 6.5° C and mean precipitation was 576 mm (1980-2010).

2.2 Instrumentation

In this study, eight CH_4 chambers are used: three chambers (T1-T3) were located in the thinned section, and five (U1-U5) were located in the undisturbed section of the forest. In areas of higher water table, CH_4 exchanges were measured, using a single ‘floating’ chamber positioned on standing shallow water in the thinned section of the forest.

Due to equipment limitations, measurements were conducted at one section at a time and were averaged from hourly chamber measurements to daily periods from 1 August to 30 September 2009 at the thinned plot, and 7 July to 30 September 2010 at the undisturbed plot. The soil chambers each had a volume of 110 l and covered a surface-area of 0.2 m^2. Concentrations in the chambers were measured for 6 minutes after chamber closure with a high precision off-axis integrated cavity output spectroscopy laser gas-analyser (DLT-100, Los Gatos Research). A small fan was installed in each chamber to ensure proper headspace mixing during closure. Air was circulated between the chamber and a manifold at a flow rate of 8-10 l min^{-1}. A sub-sample of the air stream was passed through the gas analyzer at a flow rate of 1.2 l min^{-1}. The rate of change in CH_4 concentration was determined through a linear fit to the first 2 minutes of concentration data and averaged over hourly periods. CH_4 fluxes were calculated as $F_{CH4} = \frac{dC}{dt}\frac{V}{A}$, where C (µmol m^{-3}), is molar density, V (m^3) is chamber volume and A (m^2) is the ground surface area covered by the chamber. Only measured fluxes were used for upscaling, i.e. CH_4 flux data was not gap-filled. For further details on the chamber measurements, see Sundqvist et al. (2014b). Soil temperature was measured continuously at a depth of 5 cm below the soil surface within the chambers using type-T thermocouples. Soil moisture was also measured continuously and averaged within the top 5 cm of the soil within chambers using Ml-2x ThetaProbe from DeltaT Devices and at additional positions throughout the study area.

2.3 Empirical model for upscaling of CH_4 exchange

Upscaling of soil CH_4 exchanges was derived using a multiple linear regression analyses (Draper and Smith, 1998) based on typical control variables: soil temperature, soil moisture and water table depth as they compare with hourly average chamber measurements. The resulting

174 regression model was assumed to be valid as long as the water table was greater than 5 cm below
175 the soil surface such that an oxic soil zone could enable CH_4 consumption by methanotrophs. For
176 higher water tables a median value of 40 μmol $m^{-2}h^{-1}$ obtained from the floating chamber
177 measurements was used. The mean value of the floating chamber was as large as 120μmol $m^{-2}h^{-1}$
178 due to several (>1000 μmol $m^{-2}h^{-1}$) flux values, possibly related to ebullition. Different
179 combinations of chamber measurement were tested when the empirical model was derived
180 through regression analyses. Three chambers were always used for model development while the
181 other five were used for model evaluation. The model that showed the best fit between input data
182 and regression curve and best predicted fluxes was selected for upscaling. Sensitivity analyses of
183 model parameters were made by local sensitivity analyses by varying one variable at the time
184 and keeping the other fixed (Hamby, 1994). Each parameter was changed by 20% at the time and
185 the change in the model output was quantified.
186
187 *2.4 Model input*
188 For upscaling of soil CH_4 exchange to site level, spatial information on soil moisture, water table
189 depth and soil temperature were needed as input. Daily average soil temperatures at the site were
190 relatively constant in space, hence only temporal variations in temperature were accounted (Table
191 1). Spatial information of soil moisture and water table depth were estimated using airborne-
192 LiDAR data collected in June 2011.
193 LiDAR point cloud data were first classified to ground and non-ground returns using
194 TerraScan (TerraSolid, Inc.). Ground-classified returns were rasterized using an inverse
195 distance weighted algorithm (Hopkinson et al., 2005) to generate a digital elevation model
196 (DEM) with a cell resolution of 1 m (Figure 1). A topographic wetness index (TWI) was derived

197 from the DEM (Beven and Kirkby, 1979), and used to estimate unsaturated zone soil moisture
198 according to Lin et al., (2006), Schmidt and Persson, (2003), and Western et al., (1999). Further,
199 Beldring et al., (1999) demonstrated that within some forested areas, the spatial patterns of soil
200 moisture can be estimated more accurately using topography than with other hydrological state
201 measurements, as the latter are often too variable when used with sparsely distributed
202 measurements. TWI is calculated as $TWI = \ln(A/\tan\beta)$, where A is the upslope area (m^2) being
203 drained through the position of interest, and β is the slope angle (degrees) of that position
204 (Beven and Kirkby, 1979). In the present study, the flow routing and the drainage area (A) have
205 been calculated in a multiple flow direction algorithm that takes the shape of the slope into
206 account (Pilesjö et al., 1998; 2006). TWI was converted to soil moisture based on the linear
207 regression between TWI and soil moisture measured at 12 site locations in 2010 (Figure 2). TWI
208 was also compared with soil moisture measured in 2013 as a separate evaluation of TWI as a
209 proxy for soil moisture at the site. Soil moisture data in 2013 were sampled at several positions
210 as oppose to other years (Figure 2).
211 The DEM was also used to estimate the spatial variability of water table depths based on
212 the assumption that topographically low areas are likely to have water table depths nearer to the
213 surface than topographically higher positions (e.g. Lamb et al., 2001, Molénat et al., 2005,
214 Seibert et al., 1997).
215 Since continuous measurements of water table depth were available only at a single location in
216 the study area a smoothed ground surface was used to represent the water table. The smoothened
217 ground surface area was lowered in each cell with the water table depth obtained from the one
218 measurement location. The elevation values' spatial autocorrelation were plotted in semi-
219 variograms in which the spatial dependency of elevation was estimated. The geomorphology of

220 the area was studied in aerial imagery and within the DEM. The average measure from valley
221 bottom to hilltop to valley bottom of the ground surface and the results of the spatial auto-
222 correlation formed the base of the smoothing process. The smoothened ground surface was
223 obtained by applying a low-pass filter that averaged the elevation values up to a distance where
224 the spatial auto-correlation of elevation declined.

225 Validation of the spatial distribution of the depth to water table and soil moisture was
226 determined using LiDAR-derived vegetation heights as a proxy indicator, assuming that trees are
227 often not as tall in wet soils compared to drier soils (Heiskanen and Makitalo, 2002; Koslowski,
228 1997; Polacek et al., 2006). Spatial variations in tree heights were determined using a digital
229 surface model (DSM) derived from LiDAR data. The DSM was determined by gridding the
230 maximum height of classified non-ground laser pulse returns within a 3 meter search radius and
231 subtracted from the DEM to determine vegetation height relative to ground surface. The
232 comparison between tree height and depth to water table and soil moisture could be made for an
233 area within 250 m radius from the tower where the trees are the same age.

234

235 *2.5 Gradient measurements*

236

237 Gradients were measured between 31.7m and 58.5 m, and between 31.7 m and 101.6 m at the main tower
238 at Norunda with a laser gas analyser (DLT-100, Los Gatos Research). Here we used the gradient
239 measured between 31.7 m and 58.5 m since footprint analyses using the model by Kljun et al (2004)
240 showed that these levels were more representative for the upscaled area than the gradient including the
241 highest level (Sundqvist et al., 2015). Tower CH_4 fluxes were calculated in two different ways; the
242 combined eddy covariance and gradient method (ECG) and the modified Bowen-ratio method (BR)

(Sundqvist et al., 2015). In the ECG method the CH4 flux is calculated according to Ficks law of diffusion:

$$F_{CH4}(ECG) = -\frac{1}{V} K_c \frac{\Delta C}{\Delta z} \quad (1)$$

where V ($m^3 mol^{-1}$) is the volume of one mole of air and C is CH_4 concentration (μmol mol^{-1}). The turbulent diffusivity Kc is derived from the Monin Obukhov similarity theory,

$$K_c = \frac{k u_* \Delta z}{\ln \frac{z_2}{z_1} - \psi_t\left(\frac{z_2}{L}\right) + \psi_t\left(\frac{z_1}{L}\right) - \int_z^{z^*} \Phi_t (1 - \phi_t) \frac{dz}{z}} \quad (2)$$

where $k = 0.4$ is von Karman's constant, u_* (m s^{-1}) is friction velocity, z_2 (m) is upper air intake height, z_1 (m) is lower air intake height, Δz is the difference between the intake heights, L is the Obukhov length and ψ_t is the diabatic correction function for heat profiles according to Högström (1988). u_* and L were obtained from the eddy covariance measurements. The function Φ_t denotes the diabatic correction function for gradients. Φ_t is integrated from the height z inside the roughness sublayer to the top of the roughness sublayer ($z_* = 35.9$ m). The roughness sublayer effects are expressed through ϕ_t (Mölder et al., 1999; Physick and Garratt, 1995). All heights take the displacement height into account.

The modified Bowen ratio method is based on the assumption of identical diffusivities for CO_2 and CH_4 fluxes. If the CO_2 flux (F_{CO2}) is known, e.g., the CH_4 exchange F_{CH4} can be derived (Moncrieff et al., 1997) as

$$F_{CH4}(BR) = F_{CO2} \frac{\Delta C_{CH4}}{\Delta C_{CO2}} \quad (3)$$

A measurement uncertainty was calculated for each half hourly value based on estimated uncertainty in the ingoing variables. Assuming independence between the errors, the error in the mean value for the investigated period was propagated according to the simplified method (Hu, 1966) for both the ECG and BR methods. The statistical uncertainty was calculated as the standard error of the mean. The total error in the mean was estimated as the sum of these uncertainties.

3. Results

3.1 Empirical model

The combination of chamber data used for developing the model had a clear impact on the goodness of fit of the empirical model (Table 2). This was also the case for the correlation between modelled fluxes and fluxes from chambers used for evaluation of the model. The model with best fit (R^2) to input data and highest correlation with evaluation data (R) was chosen for upscaling of the CH_4 exchange. The model with the overall best performance had an R^2 of 0.8 and R values of 0.85, 0.72, 0.94, 0.68 and 0.15 (Table 2) for U1, U2, U5, T1 and T3, respectively. All R values except the one for T3 were significant. The model equation for estimating the net CH_4 exchange $\left(CH_{4exchange}\right)$ was $CH_{4exchange} = -0.32T + 3.5W + 0.08SM - I$, where T is soil temperature, W is water table depth, SM is soil moisture and I is the regression intercept which equaled 2.8 μmol m^{-2} h^{-1}.

Uptake values (μmol m^{-2} h^{-1}) were overestimated for U1, U5 and T3 and underestimated for U2 (Figure 3). Sensitivity analyses showed that the model was equally sensitive for changes in water table depth and soil temperature and less sensitive to changes in soil moisture. A 20 % change in parameter values resulted in 9.1%, 9.2% and 2.7 % change in net CH_4 exchange for water table depth, soil temperature and soil moisture, respectively.

3.2 TWI and soil moisture

TWI and soil moisture were positively correlated with R values ranging from 0.1-0.7 in 2013 and 0.2-0.7 in 2010 (Figures 4a-b). The correlation coefficients were higher on average in 2013 (Figure 4a). Correlations were not significant due to the limited number of soil moisture

291 measurements. P-values for 2010 were generally < 0.2 (Figure 4c). When soil moisture
292 decreased after precipitation, the correlation between TWI and soil moisture increased slightly
293 (Figure 4d). Spatio-temporal variability in soil moisture generated from the relationship between
294 TWI and soil moisture measurements was on average between 14.7- 22.3 % for 96 % of the data
295 (Figure 5a). Daily input data from soil moisture measurements varied between 5-35 %. A map of
296 tree heights in the study area is shown in Figure 5b. It can be seen that areas with lower than
297 average tree heights coincide with areas with higher than average soil moisture in the area within
298 250 m radius from the tower were trees are the same age. There was a significant correlation
299 between soil moisture and tree height with a correlation coefficient of -0.16.
300
301 *3.3 Water table depth*
302 For each 1 m by 1 m cell, the spatial dependency of elevation on the water table was estimated to
303 be 80 m. A water table surface was generated applying a low-pass filter on the DEM that
304 averaged the elevation values taking 80 m surroundings into account. The ground water
305 measurements were used to let this filtered water table fluctuate temporarily. Spatio-temporal
306 variability in water table ranged on average from -5 m below ground to 0.7 m above ground if
307 excluding outliers, with 2 and 98 percentiles of -2.9 m and -0.27 m. A few wet patches with
308 standing water are shown in the map of modelled water table depth averaged over the study time
309 period (Figure 5c). In figure 5b it can be seen that in areas within 250 m from the tower, lower
310 than average tree heights coincide with areas with higher than average water tables. There was a
311 significant correlation between depth to water table and tree height with a correlation coefficient
312 of -0.29.
313

314

315 *3.4 Upscaled CH_4 exchange*

316 Averaged modelled net CH_4 exchange (derived as described in Section 2.2) of the entire study
317 area and time period is -10.0 µmol m^{-2} h^{-1} with a standard deviation of 0.8 µmol m^{-2} h^{-1}.
318 However, the average CH_4 exchange for the entire measurement period varies spatially between
319 uptake values of -21 µmol m^{-2} h^{-1} and the assigned production value of 40 µmol m^{-2} h^{-1} for areas
320 with standing water (Figure 5d). Net average emissions are found for 1.75% of the study area.
321 Time series of daily averaged modelled CH_4 exchange, soil moisture, soil temperature and water
322 table depth are shown in Figure 6. Over the course of the measurement period, net CH_4 uptake
323 decreased along with decreased soil temperatures.

324

325

326

327

328

329

330

331

4. Discussion

4.1 Evaluation of model and upscaling

Although the empirical model for upscaling of CH_4 exchange only includes data from three chamber locations and is driven by the three variables, soil temperature, depth to water table and soil moisture, this method shows good agreement between modelled and measured fluxes, in general. However the model is unsuccessful in capturing local deviations in CH_4 flux behavior such as the peak emission followed by a shift from source to sink of chamber T3 (Figure 3). The peak in CH_4 emissions may be due to high soil moisture level following precipitation (Sundqvist et al., 2014b), with the shift to a sink when the soil dries up.

Since the model is less sensitive to changes in soil moisture than to changes in water table depth and soil temperature (cf.Eq.1), soil moisture driven events might not be fully captured.

Modelled estimates of soil moisture and water table depths derived from LiDAR data agrees well with the qualitative picture we have of the study area. Moreover, the shorter trees are found in areas with higher soil moisture and near surface water table, which support the hydrological patterns generated from the DEM (Heiskanen and Makitalo, 2002; Koslowski, 1997; Polacek et al., 2006). Future studies should include more measurements of soil moisture and water table depths covering a larger area for a more quantitative evaluation. It would also be desirable to evaluate the upscaling by measuring CH_4 fluxes with soil chambers at several locations in the area.

4.2 Upscaled CH_4 exchange

The results of the modelled/upscaled soil CH_4 exchange indicates that this forest is an overall sink of -10.0 μmol $m^{-2}h^{-1}$. Even if the assigned production areas of 40 μmol $m^{-2}h^{-1}$ (for water

356 table depths higher than 5 cm below the soil surface) were extended to all water table depths
357 higher than 30 cm below the soil surface, the area remained a net sink of -9.1 μmol $m^{-2}h^{-1}$.
358 According to the chamber measurements, the average CH_4 exchange for the undisturbed forest
359 and the thinned forest were -10 μmol m^{-2} h^{-1} and -5μmol m^{-2} h^{-1}, respectively (Sundqvist et al.,
360 2014b), and hence agreed well with the modelled values. Results from the modelled site-wide
361 water table depth show that 90 % of the area had a water table lower than -0.7 m, which should
362 be well below the critical levels for net CH_4 emissions. Christiansen et al. (2012) found that
363 maintaining a ground water table depth below 0.5 m throughout their study area would shift their
364 site from a source of CH_4 to a sink of CH_4. Assuming that an uptake of -10 μmol $m^{-2}h^{-1}$ is
365 reasonable in well aerated soils, a net production area of more than 20 % of the total area, with
366 average fluxes of 40 μmol $m^{-2}h^{-1}$, would be necessary to shift the site from a sink to a source.
367 The size of this area would of course decrease if the CH_4 production rates approached levels of
368 wetland fluxes. In general, uptake rates decreased from July to September (Figure 6) and it is
369 possible that additional data from wetter and colder seasons would alter the findings.
370
371 *4.3 Water table depth*
372 We used filtered elevation data derived from LiDAR measurements to derive the general pattern
373 of the water table in the study area and regulated the absolute depths of the modelled water table
374 with measurements from one single location. Other studies have modelled water tables from
375 TWI, which may be related to topography, depending on soil type (Buttle et al. 2004). Siebert et
376 al. (1997) concluded that one single location of observation of water table depth was sufficient
377 for the calibration of an index to predict groundwater spatially distributed in a spruce forested
378 catchment in the West of Sweden. However, we are aware of an area with standing water in

summer 2010, which was not accurately captured by the model, although the generated water table map and soil moisture map show higher than average values for this area. The generation of the water table depth is based solely on the DEM. In nature, water table depth is also dependent on soil properties such as large pore structure, impermeable clay layers and sub-surface lateral flow in hillslopes (Grip and Rodhe, 1994; Ward and Trimble, 2004). Clay layers in Norunda soils have been observed at a few locations, but their spatial extent and general depth are unknown.

Moreover, the water table map was developed under conditions where the observed water table depth ranged from 0.9 m-1.7m below soil surface. Jungkunst et al. (2008) found that CH_4 emissions of a hydromorphic forest soil increased drastically when the water table was 10-20 cm from the soil surface. Fiedler and Sommer (2000) determined a threshold depth of 15 cm of the water table for wetland soils; above this threshold, production dominated the CH_4 exchange. Since the control of CH_4 production at high water tables differs from drivers of CH_4 consumption and mainly depends on substrate availability and soil temperature (Christensen et al., 2003), an additional model developed for high water tables might improve the upscaling.

4.4 Soil moisture

Observed soil moisture was well represented by the model with variations between 5% and 35%. However, the average spatial variation of soil moisture generated from TWI was lower. The porosity of the soil in Norunda is around 40% and in areas with standing water, soil moisture should reach the value of the porosity. Only 0.5 % of the cells had average soil moisture above 24% and no cells had average values above 31%. These low values may point to the fact that wet areas with observed standing water were situated in parts of the landscape which are represented

as flat or convex in the DEM. The water routing algorithm creates a pattern, which is based only on the topography. The model might then disperse water over larger areas rather than concentrating it due to low differences in elevation values. In reality, however, micro-topography and soil properties may drive the water distribution.

4.5 Upscaling soil CH_4 exchange versus gradient measurements

The results from upscaling of soil CH_4 exchange show a net consumption of about -10 μmol $m^{-2}h^{-1}$while the tower gradient measurement indicates the site is a net CH_4 source of about 3.4 μmol $m^{-2}h^{-1}$ for the same time period (Sundqvist et al.,2015). The ECG method resulted in a mean emission of 5.2 ± 0.64 μmol $m^{-2}h^{-1}$ while the BR method gave 1.6 ± 0.73 μmol $m^{-2}h^{-1}$. The errors of these two methods does not overlap but both indicate that the forest is a source of methane. The difference between the methods is most likely caused by uncertainty in the methods itself. Here are many empirical corrections involved especially in the ECG method that might be the cause of this discrepancy.

Unfortunately the uncertainty in the upscaled soil emissions cannot be easily done since we do not have enough spatial data on e.g. soil properties available. The rough sensitivity analyses made in section 4.2 is however a strong indication that the soil is a sink of methane and not a source.

The study area included the outskirts of a clear-cut (Figure 2). The water table in this part of the study area was increased due to decreased evapotranspiration following clear-cutting. The model did not capture this local effect since water table depth was calculated from elevation data and a single measurement location within the forest. Chamber measurements on the clear-cut from October -November 2010 showed average emissions of 15 μmol $m^{-2}h^{-1}$ (Sundqvist et al.,

2015). Emissions from the clear-cut may be part of the reason for the discrepancy between the upscaled soil chamber data and the gradient measurements. It is also possible that emissions from the part of the clear-cut located outside of the upscaled boundary and other sources outside the study area contribute to the tower gradient measurements.

The gradient measurements represent the net exchange of CH_4 above the canopy and hence it is not possible to distinguish fluxes at soil level from an exchange of CH_4 coupled to vegetation. CH_4 emissions by vegetation (Terazawa et al. 2007; Gauci 2010; Keppler et al. 2006; Vigano et al. 2008) could partly explain the discrepancy between upscaled chamber data and gradient measurements, if these contribute significantly to the net CH_4 exchange at Norunda. However, so far only a net uptake of CH_4 by vegetation has been measured at a few locations at Norunda (Sundqvist et al. 2012).

5 Conclusions

A simple empirical model for upscaling of soil CH_4 exchange at a boreal forest site was developed from chamber measurements, driven by soil temperature, water table depth and soil moisture. High resolution LiDAR elevation data formed the basis for the mapping of water table depth and soil moisture of the study area, while vegetation heights were used as a proxy indicator for spatial variations of average soil moisture regime. A significant correlation was found between the topographical wetness index (TWI) derived from the LiDAR data and soil moisture measured at the study area, which enabled a conversion of TWI to soil moisture. Modelled CH_4 fluxes were in good agreement with measured fluxes at four out of five chamber locations used for evaluation. An improvement of the model could be achieved by a better representation of high water tables. The results from upscaling of CH_4 exchange show a net uptake of CH_4 of -10

448 μmol $m^{-2}h^{-1}$. This is in contrast to gradient measurements above the canopy in the center of the
449 study area, which yielded net CH_4 emissions for the same time period (Sundqvist et al., 2015).
450 Emissions were only found from 1.75 % of the surface of the study area. This suggests that the
451 net emissions measured by the tower gradient method above the tree canopy probably originated
452 from sources outside the study area and possibly also from CH_4 emissions by the vegetation.
453

Acknowledgements

Support for this work was provided by Formas, by the Linnaeus Centre LUCCI (http://www.lucci.lu.se/index.html) funded by the Swedish Research Council and by the EU project InGOS. We thank Anders Båth and Irene Lehner for field assistance. Airborne LiDAR for the Norunda site was acquired with support from the British Natural Environment Research Council (NERC/ARSF/FSF grant EU10-01 and NERC/GEF grant 933).

463 **References**

464 Beldring, S., Gottschalk, L., Seibert, J., and Tallaksen, L.M., 1999, Distribution of soil moisture
465 and groundwater levels at patch and catchment scales: Agricultural and Forest Meteorology, v.
466 98–99, p. 305-324.
467
468 Beven, K.J., and Kirkby, M.J., 1979, A physically based, variable contributing area model of
469 basin hydrology: Hydrol.Sci.Bull, v. 24, p. 43-69.
470
471 Boeckx, P., VanCleemput, O., and Villaralvo, I., 1997, Methane oxidation in soils with different
472 textures and land use: Nutrient Cycling in Agroecosystems, v. 49, p. 91-95.
473
474 Buttle, J. M., P. J. Dillon, and G. R. Eerkes, 2004. Hydrologic coupling of slopes, riparian zones
475 and streams: an example from the Canadian Shield. Journal of Hydrology 287:161-177
476
477 Castro, M.S., Melillo, J.M., Steudler, P.A., and Chapman, J.W., 1994, Soil-miosture as a
478 predictor of methane uptake by temeprate forest soils: Canadian Journal of Forest Research-
479 Revue Canadienne De Recherche Forestiere, v. 24, p. 1805-1810.
480
481 Christensen, T.R., Ekberg, A., Strom, L., Mastepanov, M., Panikov, N., Oquist, M., Svensson,
482 B.H., Nykanen, H., Martikainen, P.J., and Oskarsson, H., 2003, Factors controlling large scale
483 variations in methane emissions from wetlands: Geophysical Research Letters, v. 30.
484

485 Christiansen, J.R., Vesterdal, L., and Gundersen, P., 2012, Nitrous oxide and methane exchange
486 in two small temperate forest catchments-effects of hydrological gradients and implications for
487 global warming potentials of forest soils: Biogeochemistry, v. 107, p. 437-454.
488
489 Crill, P.M., Martikainen, P.J., Nykanen, H., and Silvola, J., 1994, Temperature and N-
490 fertilization effects on methane oxidation in a drained peatland soil: Soil Biology &
491 Biochemistry, v. 26, p. 1331-1339.
492
493 Curry, C.L., 2007, Modeling the soil consumption of atmospheric methane at the global scale:
494 Global Biogeochemical Cycles, v. 21.
495
496 Del Grosso, S.J., Parton, W.J., Mosier, A.R., Ojima, D.S., Potter, C.S., Borken, W., Brumme, R.,
497 Butterbach-Bahl, K., Crill, P.M., Dobbie, K., and Smith, K.A., 2000, General CH4 oxidation
498 model and comparisons of CH4 oxidation in natural and managed systems: Global
499 Biogeochemical Cycles, v. 14, p. 999-1019.
500
501 Dorr, H., Katruff, L., and Levin, I., 1993, Soil texture parameterization of the methane uptake in
502 aerated soils: Chemosphere, v. 26, p. 697-713.
503
504 Draper, N.R., and Smith, H., 1998, Applied Regression analyses, Wiley-Interscience, 307-312 p.
505

506 Dunfield, P., Knowles, R., Dumont, R., and Moore, T.R., 1993, Methane production and
507 consumption in temperate and sub-arctic peat soils-response to temperature and pH: Soil Biology
508 & Biochemistry, v. 25, p. 321-326.
509
510 Dutaur, L., and Verchot, L.V., 2007, A global inventory of the soil CH(4) sink: Global
511 Biogeochemical Cycles, v. 21.
512
513 Fiedler, S., Holl, B.S., and Jungkunst, H.F., 2005, Methane budget of a Black Forest spruce
514 ecosystem considering soil pattern: Biogeochemistry, v. 76, p. 1-20.
515
516 Fiedler, S., and Sommer, M., 2000, Methane emissions, groundwater levels and redox potentials
517 of common wetland soils in a temperate-humid climate: Global Biogeochemical Cycles, v. 14, p.
518 1081-1093.
519
520 Fischer, J.C.v., and Hedin, L.O., 2002, Separating methane production and consumption with a
521 field-based isotope pool dilution technique: Global Biogeochemical Cycles, v. 16, p. 8/1-8/13.
522
523 Gauci, V., Gowing, D.J.G., Hornibrook, E.R.C., Davis, J.M., and Dise, N.B., 2010, Woody stem
524 methane emission in mature wetland alder trees: Atmospheric Environment, v. 44, p. 2157-2160.
525
526 Grayson, R.B., Western, A.W., Chiew F.H.S., 1997. Preferred states in spatial soil moisture
527 patterns: Local and nonlocal controls. Water Resources Research 33: 2897–2908.
528

529 Grip, H., and Rodhe, A., 1994, Vattnets väg från regn till bäck: Uppsala, Hallgren & Fallgren
530 Studieförlag AB.
531
532 Grunwald, D., Fender, A.C., Erasmi, S., and Jungkunst, H.F., 2012, Towards improved bottom-
533 up inventories of methane from the European land surface: Atmospheric Environment, v. 51, p.
534 203-211.
535
536 Guckland, A., Flessa, H., and Prenzel, J., 2009, Controls of temporal and spatial variability of
537 methane uptake in soils of a temperate deciduous forest with different abundance of European
538 beech (Fagus sylvatica L.): Soil Biology & Biochemistry, v. 41, p. 1659-1667.
539
540 Hamby, D.M., 1994, A review of techniques for parameter sensitivity analysis of environmental
541 models: Environmental Monitoring and Assessment, v. 32, p. 135-154.
542
543 Harriss, R.C., Sebacher, D.I., and Day, F.P., 1982, Methane flux in the great dismal swamp:
544 Nature, v. 297, p. 673-674.
545
546 Hashimoto, S., Morishita, T., Sakata, T., Ishizuka, S., Kaneko, S., and Takahashi, M., 2011,
547 Simple models for soil CO2, CH4, and N2O fluxes calibrated using a Bayesian approach and
548 multi-site data: Ecological Modelling, v. 222, p. 1283-1292.
549

Heiskanen, J., and Makitalo, K., 2002, Soil water-retention characteristics of Scots pine and Norway spruce forest sites in Finnish Lapland: Forest Ecology and Management, v. 162, p. 137-152.

Hopkinson, C., Chasmer, L.E., Sass, G., Creed, I.F., Sitar, M., Kalbfleisch, W., and Treitz, P., 2005, Vegetation class dependent errors in lidar ground elevation and canopy height estimates in a boreal wetland environment: Canadian Journal of Remote Sensing, v. 31, p. 191-206.

Högstrom, U., 1988, Non-dimensional wind and temperature profiles in the atmospheric surface-layer- a re-evaluation:Boundary layer meteorology, **42**, 55-78.

Ku, H. H., 1966, Notes on the use of propagation of error formulas: Journal of Research of the National Bureau of Standards (National Bureau of Standards) 70C (4): 262. doi:10.6028/jres.070c.025. ISSN 0022-4316

Ishizuka, S., Sakata, T., Sawata, S., Ikeda, S., Sakai, H., Takenaka, C., Tamai, N., Onodera, S., Shimizu, T., Kan-na, K., Tanaka, N., and Takahashi, M., 2009, Methane uptake rates in Japanese forest soils depend on the oxidation ability of topsoil, with a new estimate for global methane uptake in temperate forest: Biogeochemistry, v. 92, p. 281-295.

Jungkunst, H.F., Flessa, H., Scherber, C., and Fiedler, S., 2008, Groundwater level controls CO(2), N(2)O and CH(4) fluxes of three different hydromorphic soil types of a temperate forest ecosystem: Soil Biology & Biochemistry, v. 40, p. 2047-2054.

573

574 Kammann, C., Grunhage, L., Jager, H.J., and Wachinger, G., 2001, Methane fluxes from
575 differentially managed grassland study plots: the important role of CH4 oxidation in grassland
576 with a high potential for CH4 production: Environmental Pollution, v. 115, p. 261-273.

577

578 Kammann, C., Hepp, S., Lenhart, K., and Mulller, C., 2009, Stimulation of methane
579 consumption by endogenous CH4 production in aerobic grassland soil: Soil Biology &
580 Biochemistry, v. 41, p. 622-629.

581

582 King, G.M., and Adamsen, A.P.S., 1992, Effects of temperature on methane consumption in a
583 forest soil and in pure cultures of the methanotroph methylomonas-rubra: Applied and
584 Environmental Microbiology, v. 58, p. 2758-2763.

585

586 Kirschke, S., 2013, Three decades of global methane sources and sinks: Nature geoscience, v. 6,
587 p. 813-823.

588

589 Kljun, N., P. Calanca, M.W. Rotach, H.P. Schmid, 2004: A Simple Parameterisation for Flux
590 Footprint Predictions. Boundary-Layer Meteorology v.112, p.503-523.

591

592 Konda, R., Ohta, S., Ishizuka, S., Arai, S., Ansori, S., Tanaka, N., and Hardjono, A., 2008,
593 Spatial structures of N(2)O, CO(2), and CH(4) fluxes from Acacia mangium plantation soils
594 during a relatively dry season in Indonesia: Soil Biology & Biochemistry, v. 40, p. 3021-3030.

595

596 Koslowski, T.T., 1997, Responses of woody plants to flooding and salinity. Tree Physiology
597 Monograph No. 1: Victoria, Canada., Heron Publishing.
598
599 Lamb, R., Beven, K., and Myrabø, S., 2001, Shallow Groundwater Response at Minifelt, *in*
600 Grayson, R., and Blöschl, G., eds., Spatial patterns in catchment hydrology, Cambridge
601 University Press, p. 272-303.
602
603 Lessard, R., Rochette, P., Topp, E., Pattey, E., Desjardins, R.L., and Beaumont, G., 1994,
604 Methane and carbon-dioxide fluxes from poorly drained adjacent cultivated and forest sites:
605 Canadian Journal of Soil Science, v. 74, p. 139-146.
606
607 Lin, H.S., Kogelmann, W., Walker, C., and Bruns, M.A., 2006, Soil moisture patterns in a
608 forested catchment: A hydropedological perspective: Geoderma, v. 131, p. 345-368.
609
610 Marushchak, M.E., Kiepe, I., Biasi, C., Elsakov, V., Friborg, T., Johansson, T., Soegaard, H.,
611 Virtanen, T., and Martikainen, P.J., 2013, Carbon dioxide balance of subarctic tundra from plot
612 to regional scales: Biogeosciences, v. 10, p. 437-452.
613
614 Matson, P.A., Vitousek, P.M., and Schimel, D.S., 1989, Regional extrapolations of trace gas flux
615 based on soils and ecosystems, John Wiley, Dahlem Koferenzen;.
616
617 McNamara, N.P., Chamberlain, P.M., Piearce, T.G., Sleep, D., Black, H.I.J., Reay, D.S., and
618 Ineson, P., 2006, Impact of water table depth on forest soil methane turnover in laboratory soil

cores deduced from natural abundance and tracer C-13 stable isotope experiments: Isotopes in Environmental and Health Studies, v. 42, p. 379-390.

Molénat, J., Gascuel-Odoux, C., Davy, P., and Durand, P., 2005, How to model shallow water-table depth variations: the case of the Kervidy-Naizin catchment, France: Hydrological Processes, v. 19, p. 901-920.

Moncrieff, J. B., Massheder, J.M., de Bruin, H., Elbers, J., Friborg, 1997, A system to measure surface fluxes of momentum, sensible heat, water vapor and carbon dioxide. Journal of hydrology **188-189**, 589-611.

Mölder, M., Grelle, A., Lindroth, A., and Halldin, S., 1999, Flux-profile relationships over a boreal forest - roughness sublayer corrections: Agricultural and forest meteorology, **98-9**, 645-658.

Nicoloni, G., Castaldi, S., Fratini, G., and Valentini, R., 2013, A literature overview of micrometeorological CH4 and N2O flux measurements in terrestrial ecosystems: Atmospheric Environment, v. 81, p. 311-319.

Physick, W.L., and Garratt, J.R., 1995, Incorporation of a high-roughness lower boundary into a mesoscale model for studies of dry deposition over complex terrain: Boundary layer meteorology, **74**, 55-71.

643 Pilesjö, P., Persson, D.A., and Harrie, L., 2006, Digital Elevation Data for Estimation of
644 Potential Wetness in Ridged Fields - Comparison of Two Different Methods: Agricultural Water
645 Management, v. 79, p. 225-247.
646
647 Pilesjö, P., Zhou, Q., and Harrie, L., 1998, Estimating flow distribution over digital elevation
648 models using a form-based algorithm: Geographic Information Sciences, v. 4, p. 44-51.
649
650 Polacek, D., Kofler, W., and Oberhuber, W., 2006, Radial growth of Pinus sylvestris growing on
651 alluvial terraces is sensitive to water-level fluctuations: New Phytologist, v. 169, p. 299-308.
652
653 Reay, D.S., Nedwell, D.B., McNamara, N., and Ineson, P., 2005, Effect of tree species on
654 methane and ammonium oxidation capacity in forest soils: Soil Biology & Biochemistry, v. 37,
655 p. 719-730.
656
657 Ridgwell, A.J., Marshall, S.J., and Gregson, K., 1999, Consumption of atmospheric methane by
658 soils: A process-based model: Global Biogeochemical Cycles, v. 13, p. 59-70.
659
660 Riley, W. J., Subin, Z.M., Lawrence, D.M., Swenson, S.C., Torn, M.S., Meng, L., Mahowald, N.M., and
661 Hess, P., 2011, Barriers to predicting changes in global terrestrial methane fluxes: analyses using
662 CLM4Me, a methane biogeochemistry model integrated in CESM. Biogeosciences 8:1925-1953.
663
664 Roulet, N., Moore, T., Bubier, J., and Lafleur, P., 1992, Northern fens-,methane flux and
665 climatic-change: Tellus Series B-Chemical and Physical Meteorology, v. 44, p. 100-105.
666

667 Schimel, D.S., and Potter, C.S., 1995, Process modelling and spatial extrapolation *in* Matson,
668 P.A., and Harriss, R.C., eds., Biogenic trace gases: Measuring emissions from soils and water:
669 Cambridge, Blackwell Sci.,, p. 358-383.
670
671 Schmidt, F., and Persson, A., 2003, Comparison of DEM Data Capture and Topographic
672 Wetness Indices: Precision Agriculture, v. 4, p. 179-192.
673
674 Seibert, J., Bishop, K.H., and Nyberg, L., 1997, A test of TOPMODEL'a ability to predict
675 spatially distributed groundwater levels: Hydrological Processes, v. 11, p. 1131-1144.
676
677 Steudler, P.A., Bowden, R.D., Melillo, J.M., and Aber, J.D., 1989, Influence of nitrogen-
678 fertilization on methane uptake in temperate forest soils: Nature, v. 341, p. 314-316.
679
680 Sundqvist, E., Crill, P., Molder, M., Vestin, P., and Lindroth, A., 2012, Atmospheric methane
681 removal by boreal plants: Geophysical Research Letters, v. 39.
682
683 Sundqvist, E., Mölder, M., Crill, P., Kljun, N., and Lindroth, A., Methane exchange in a boreal
684 forest estimated by gradient method, Tellus B, 2015, 67, 26688,
685
686 Sundqvist, E., Vestin, P., Crill, P., Persson, T., and Lindroth, A., 2014b, Short-term effects of
687 thinning, clear-cutting and stump harvesting on methane exchange in a boreal forest,
688 Biogeosciences, 11, 6095-6105
689

690 Tenenbaum, D.E., Band, L.E., Kenworthy, S.T., Tague, C.L., 2006. Analysis of soil moisture
691 patterns in forested and suburban catchments in Baltimore, Maryland, using high-resolution
692 photogrammetric and LIDAR digital elevation datasets. Hydrological
693 Processes 20: 219-240.
694
695 Tian, H., Xu, X., Liu, M., Ren, W., Zhang, C., Chen, G., and Lu, C., 2010, Spatial and temporal patterns
696 of CH4 and N2O fluxes in terrestrial ecosystems of North America during 1979-2008: application of a
697 global biogeochemistry model. Biogeosciences 7:2673-2694.
698
699 Vigano, I., van Weelden, H., Holzinger, R., Keppler, F., McLeod, A., and Rockmann, T., 2008,
700 Effect of UV radiation and temperature on the emission of methane from plant biomass and
701 structural components: Biogeosciences, v. 5, p. 937-947.
702
703 Ward, A.D., and Trimble, S.W., 2004, Environmental hydrology, Lewis publisher.
704 Weslien, P., Klemedtsson, A.K., Borjesson, G., and Klemedtsson, L., 2009, Strong pH influence
705 on N2O and CH4 fluxes from forested organic soils: European Journal of Soil Science, v. 60, p.
706 311-320.
707
708 Western, A.W., Grayson, R.B., Blöschl, G., Willgoose, G.R., and McMahon, T.A., 1999,
709 Observed spatial organization of soil moisture and its relation to terrain indices: Water Resources
710 Research, v. 35, p. 797-810.
711

712 Yu, K.W., Faulkner, S.P., and Baldwin, M.J., 2008, Effect of hydrological conditions on nitrous
713 oxide, methane, and carbon dioxide dynamics in a bottomland hardwood forest and its
714 implication for soil carbon sequestration: Global Change Biology, v. 14, p. 798-812.
715
716 Yvon-Durocher, G., Allen, P.A., Bastviken, B., Conrad, R., Gudasz, C., St-Pierre, A., Thanh-
717 Duc, N., and Giorgio, P.A., 2014, Methane fluxes show consistent temperature dependence
718 across microbial to ecosystem scales: Nature, v. 507, p. 488-491.
719
720
721 Zhuang, Q., Melillo, J.M., Kicklighter, D.W., Prinn, R.G., McGuire, A.D., Steudler, P.A., Felzer, B.S.,
722 and Hu, S., 2004, Methane fluxes between terrestrial ecosystems and the atmosphere at northern high
723 latitudes during the past century: A retrospective analysis with a process-based biogeochemistry model.
724 Global Biogeochemical Cycles 18:GB3010, doi:3010.1029/2004GB002239.

Tables

Table 1.
Soil temperature variability at Norunda. Here *Mean* and *Std* are the mean and standard deviation of the soil temperature respectively at *n* number of measurement locations within the study area. The measurements were taken in 2014.

	Mean (°C)	Std (°C)	n
July (undisturbed forest)	17.2	2.1	21
July (thinned forest)	17.9	1.4	12
September (undisturbed forest)	8.3	1.0	21
September (thinned forest)	7.8	0.9	12

744 Table 2

745 Evaluation of empirical models for upscaling of CH_4 exchange.

746 ID is the combination of chambers used for model devlopement. R^2 is the adjusted coefficient of

747 determination for the multiple linear regression analyses between model and chamber input data.

748 B(T), B(W) and B(SM) are the coefficients for soil temperature, water table depth and soil

749 moisture, respectively, obtained from the multiple linear regression analyses. I is the regression

750 intercept. R is the Pearson correlation coefficient for modelled CH_4 exchange and chamber data.

751 *) Not significant at p >0.05. n.i) Not included due to non-significance. -) Chamber was used for

752 model development and is therefore not evaluated.

753

ID	R^2	B (T)	B (W)	B (SM)	I	R (U1)	R (U2)	R (U3)	R (U4)	R (U5)	R (T1)	R (T2)	R (T3)
U4, U5, T1	0.68	-0.43	5.8	n.i	4.8	0.79	0.79	0.81	-	-	-	0.71	-0.33*
U4, U3, T1	0.80	-0.31	3.1	0.08	3.7	0.80	0.78	-	-	0.96	-	0.63	-0.43*
U4, U2, T1	0.58	-0.30	1.9	0.09	-6.3	0.85	-	0.87	-	0.94	-	0.48	0.13
U4, U2, T1	0.55	-0.42	7.2	n.i	7.2	-	0.78	0.81	-	0.94	-	0.71	-0.21*
U4, U5, T2	0.71	-0.20	2.2	0.03	-4.6	0.84	0.74	0.88	-	-	0.62	-	-0.09*
U4, U3 T2	0.80	-0.32	3.5	0.08	-2.8	0.85	0.72	-	-	0.94	0.68	-	0.15*
U4, U2, T2	0.57	-0.33	3.6	0.05	-2.4	0.84	-	0.88	-	0.96	0.62	-	-0.09*
U4, U1, T2	0.54	-0.46	6.0	n.i	5.8	-	0.79	0.81	-	0.95	0.41	-	-0.34*
U4, U5, T3	0.56	n.i	8.1	0.16	0.60	0.69	0.61	0.74	-	-	0.08	-0.03*	-
U4, U3, T3	0.54	n.i	6.8	0.22	-4.6	0.71	0.58	-	-	0.67	0.58	-0.04*	-
U4, U2, T3	0.52	0.40	4.5	0.30	-15.3	0.43	-	0.36	-	0.18*	0.47	-0.23*	-
U4, U1, T3	0.53	n.i	8.9	0.15	2.3	-	0.62	0.74	-	0.68	0.54	-0.02*	-
U5, U3, T1	0.51	-0.37	n.i	0.05	-5.9	0.81	0.66	-	0.83	-	-	0.52	-0.46*
U5, U2, T1	0.28	-0.39	n.i	0.03	-5.7	0.80	-	0.72	0.80	-	-	0.52	-0.53*
U5, U1, T1	0.58	-0.49	4.7	-0.03	5.7	-	0.79	0.73	0.82	-	-	0.62	-0.53*
U5, U3, T2	0.53	-0.39	n.i	0.06	-5.7	0.81	0.65	-	0.83	-	0.41	-	-0.42*
U5, U2, T2	0.30	-0.42	1.3	n.i	-2.7	0.78	-	0.74	0.80	-	0.19	-	-0.57*
U5, U1, T2	0.59	-0.51	2.6	n.i	2.2	-	0.75	0.77	0.83	-	0.24	-	-0.54*
U5, U3, T3	0.44	n.i	n.i	0.32	-15.1	0.64	0.44	-	0.52	-	0.59	-0.06*	-
U5, U2, T3	0.39	n.i	n.i	0.33	-16.1	0.64	-	0.51	0.52	-	0.59	-0.06*	-
U5, U1, T3	0.48	n.i	3.4	0.24	-6.9	-	0.53	0.62	0.65	-	0.60	-0.05*	-
U3, U2, T1	0.50	-0.17	2.9	0.08	6.5	0.83	-	-	0.90	0.89	-	0.31	0.53
U3, U1, T1	0.25	-0.40	-1.6	0.03	-6.7	-	0.57	-	0.67	0.80	-	0.46	-0.56*
U3, U2, T2	0.49	-0.19	4.6	0.05	-3.1	0.80	-	-	0.93	0.89	0.66	-	0.37
U3, U1, T2	0.29	-0.42	-1.8	0.05	-7.0	-	0.57	-	0.70	0.81	0.26	-	0.53
U3, U2, T3	0.53	0.35	12.0	0.21	-3.4	-0.43*	-	-	-0.49*	-0.78*	0.25	-0.39*	-
U3, U1, T3	0.37	n.i	n.i	0.30	-14.2	-	0.44	-	0.52	0.51	0.59	-0.06*	-
U2, U1, T1	0.16h	-0.44	n.i	n.i	-3.8	-	-	0.68	0.72	0.87	-	0.50	-0.59*
U2, U1, T2	0.19	-0.46	n.i	n.i	-3.5	-	-	0.68	0.72	0.87	0.13	-	-0.59*
U2, U1, T3	0.35	n.i	5.7	0.20	-4.8	-	-	0.69	0.73	0.66	0.59	-0.04*	-

754

Figures

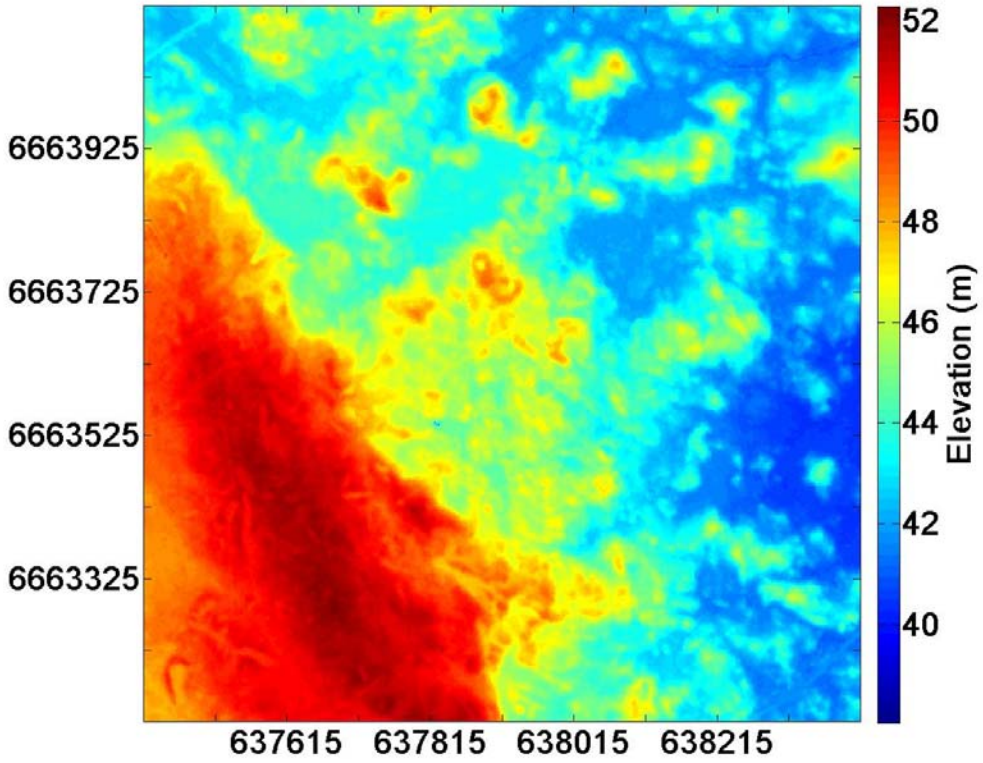

Figure 1. Digital Elevation Model (DEM) of the study area. Coordinates are given in UTM (WGS 84).

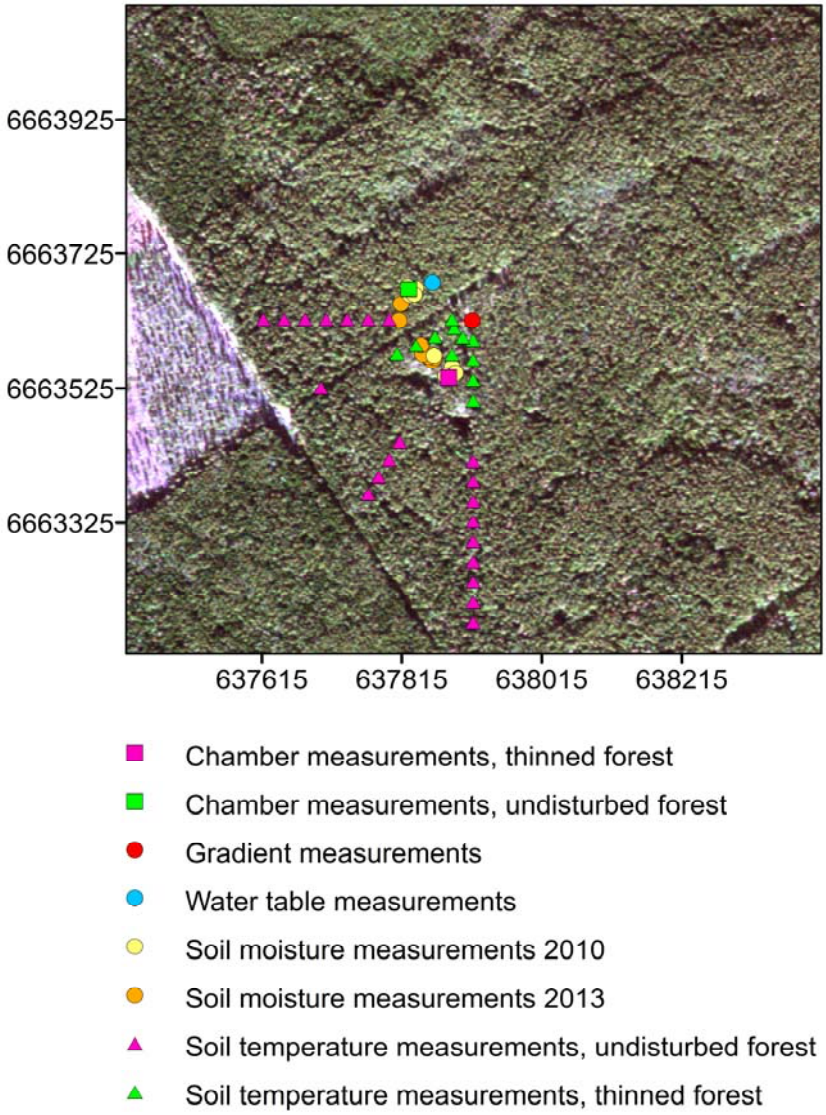

785
786
787 Figure 2. Photo of the study area showing locations for chamber measurements, soil moisture
788 measurements, water table measurements and gradient measurements. The clear-cut can be seen
789 to the left.
790 (Source: Geoeye-1© GeoEye Inc.<2009> Distributed by e-GEOS)
791
792

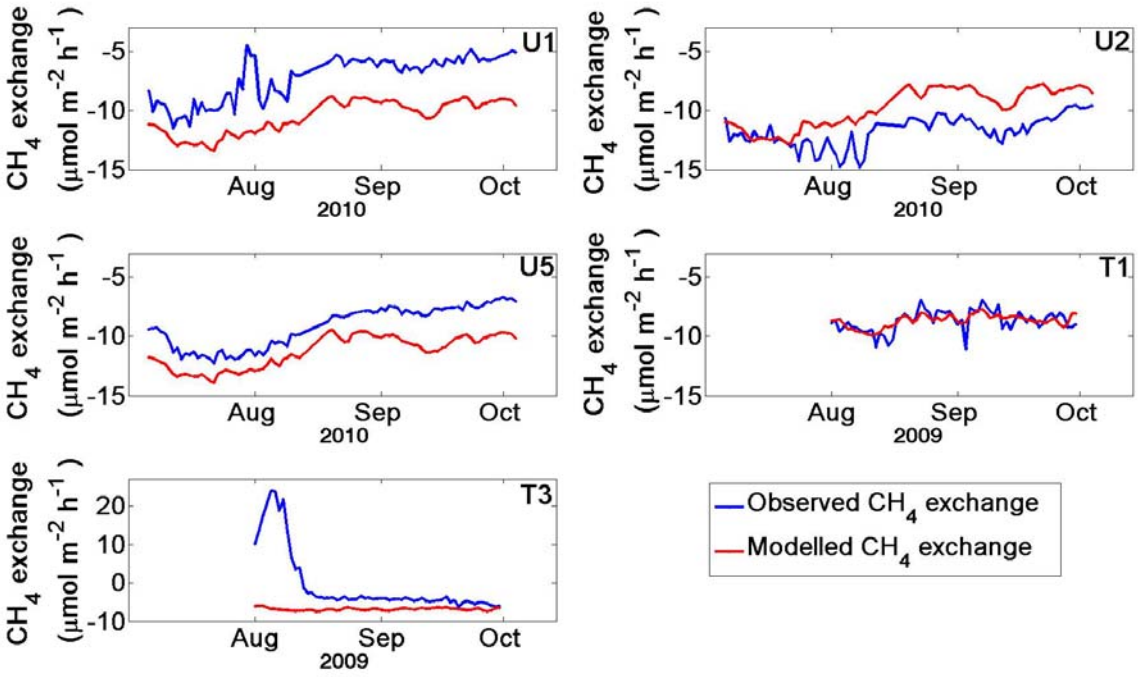

793 Figure 3. Comparison between modelled and observed CH_4 exchange for the evaluation
794 chambers. U*x* are chambers in the undisturbed forest and T*x* are chambers in the thinned forest.
795

796

797
798
799
800
801
802
803
804
805
806
807
808
809
810

811
812
813
814
815
816
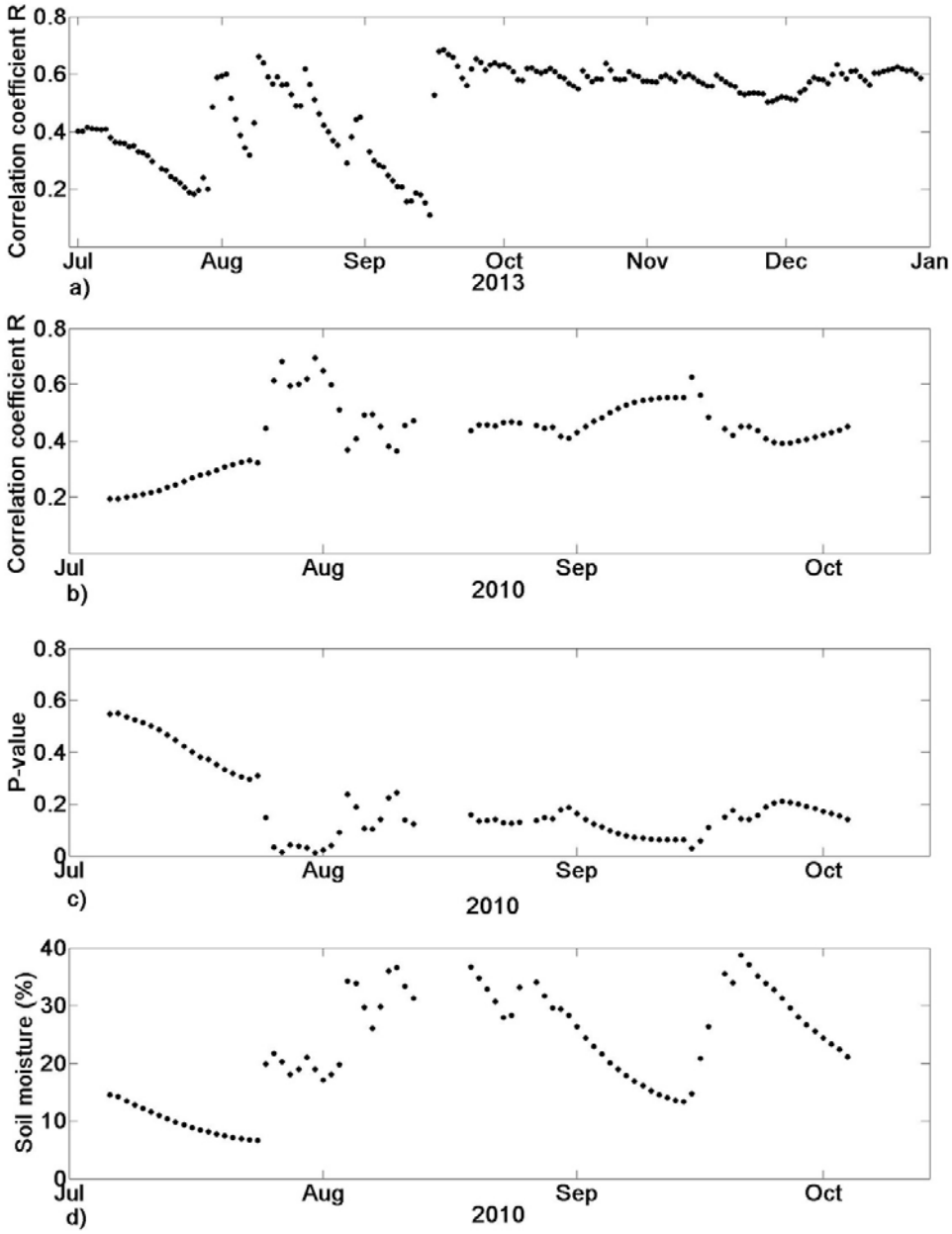

817 Figure 4. Average daily Pearson correlation between TWI and soil moisture measured at a) 9
818 locations July- December 2013; and b) 12 locations July-October 2010; Daily significance level
819 for correlations between c) TWI and soil moisture measured at 12 locations July-October 2010;
820 and d) daily soil moisture at one measurement location for the time period July-October 2010.

821

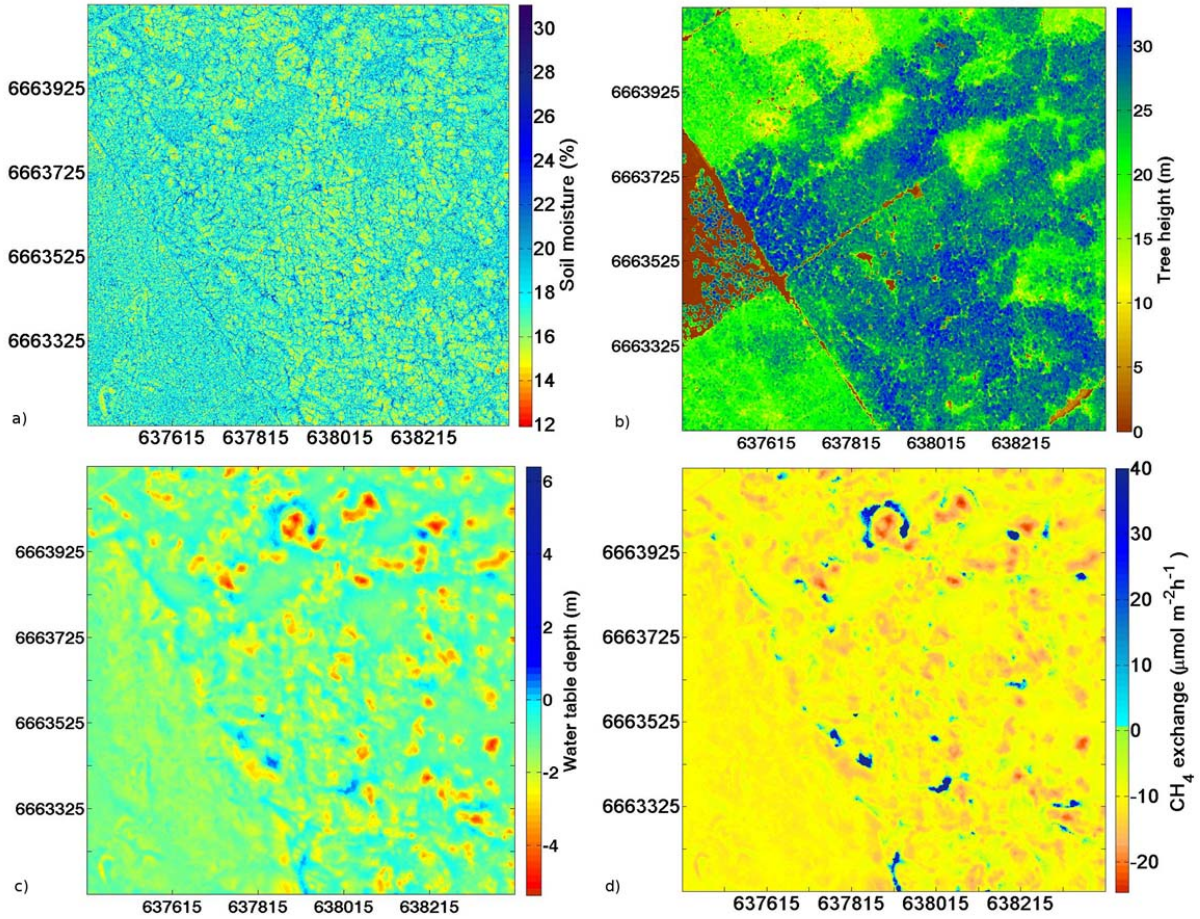

Figure 5. a) Map of soil moisture for the entire study area, averaged over the study time period July through September 2010. b) Map of tree height in the study area. c) Map of water table depth for the study area, averaged over the study time period. d) Map of modelled CH_4 exchange for the study area, averaged over the study time period. Coordinates are given in UTM (WGS 84).

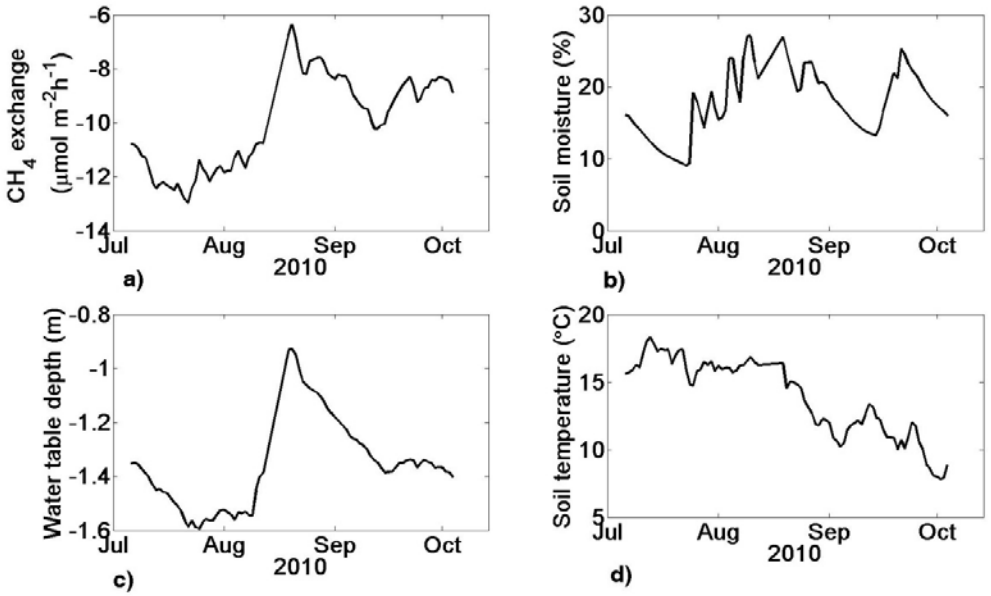

Figure 6. Time series of modelled a) CH_4 exchange, b) soil moisture, c) water table depth and d) soil temperature, spatially averaged over the study area.